

Study on the Microstructure and Mechanical Properties of Large-size Bainite Type Non-quenched and Tempered Steel

Zeyu Wu

University of Shanghai for Science and Technology, Shanghai, China

Abstract

The microstructure and mechanical properties of Bainitic untempered steel at different positions after air cooling at 1000 °C and tempering at 450 °C were studied. The Bainitic untempered steel has a diameter of 200 mm and the sample is cut equidistant from the center to the edge along the radius direction. The microstructure and mechanical properties of the large size Bainitic untempered steel were analyzed by metallographic microscope, scanning electron microscope, X-ray diffractometer, micro-Vickers hardness testing machine and electronic universal material testing machine. The results show that the microstructure of the steel is composed of granular bainite and lath bainite at different positions, with the sampling position closer to the edge, the content of lath bainite increases first and then decreases, the lath bainite becomes finer, the content of granular bainite decreases continuously, the size of M/A island and grain size decrease continuously; The results of mechanical properties test show that the tensile strength and yield strength of bainite non-quenched and tempered steel increase first and then decrease as the sampling position gets closer to the edge, and the elongation decreases first and then increases.

Keywords

Heat Treatment; Bainite Non-quenched and Tempered Steel; Sampling Location.

1. Introduction

Bainite non-quenched and tempered steel is mainly based on medium carbon steel, reducing the carbon content and adding various microalloying elements and expanding the bainite transition region (such as Mn, B, Cr, Mo, etc.), adjusting the type and quantity of added elements to obtain different strength grades^[1]. Its microstructure is generally lath-like bainite or granular bainite, in which the granular bainite is composed of a bainite ferrite matrix and M/A islands distributed on the matrix^[2]. Its tensile strength can reach around 1000 MPa or even higher^[3]. At present, it has been widely used in the construction machinery industry, vehicle industry, civil industry, marine field, etc^[4-5]. The heat treatment of bainite non-quenched and tempered steel is usually air-cooled heat treatment, which has good strength and toughness, and its mechanical properties are stronger than those of typical bainite steel and quenched and tempered steel^[6-7], however, in the process of air cooling and heat treatment, when the diameter of bainite non-quenched and tempered steel parts is large, the surface and core of the parts in the air cooling process will have uneven mechanical properties due to the difference in cooling speed^[8-9], which will affect the performance of the parts.

In the existing studies, Xian Fenqiang et al^[10] designed and developed bainitic untempered steel XGMnVS with a diameter of 175 mm. The steel structure is a mixed structure of plat bainite + granular bainite, and its comprehensive mechanical properties are good. The study of Li Monge et al^[11] showed that the test rods of bainite steel with different diameters were all bainite ferrite and residual austenite after air cooling and tempering, which belonged to the non-carbide bainite structure. The microstructure of the rods with a diameter of less than 30 mm changed little after heat treatment,

and the core structure of the rods with a diameter of more than 50 mm was coarsened, accompanied by an increase in granular bainite content. After heat treatment, the strength and hardness of the bar tend to decrease with the increase of the diameter of the bar. Wang Siqian et al^[12] studied 35CrMoV forgings with thickness of 100 mm and 140 mm, and the results showed that the mechanical properties decreased significantly from the surface to the inside, and the microstructure changed from tempered sorbite to a mixed structure of tempered sorbite and bainite. Therefore, the microstructure and mechanical properties of Bainitic untempered steel at different positions after air cooling at 950 °C and tempering at 450 °C are studied in this paper, in order to provide reference for the practical design and application of large diameter Bainitic untempered steel.

2. Experiment

2.1 Experimental Materials and Experimental Processes

In this experiment, the production process of bainite non-quenched and tempered steel bar is electric arc furnace smelting (EAF) + ladle refining (LF) + vacuum treatment (VD), and then the ladle molten steel is continuously cast and drawn into a continuous casting billet for slow cooling, then heated to 1000 °C for hot rolling, rolled into a bar with a diameter of 200 mm, and then air-cooled, after the air cooling to room temperature, the bar is heated to 450 °C tempered and insulated for 2 h, and then air-cooled. The bainite type non-quenched and tempered steel is sampled equidistant from the core to the edge along the radius direction, as shown in Figure 1, and the samples cut from the heart to the edge are numbered C-0, C-1, C-2, and C-3 in turn.

The microstructure and tensile fracture morphology of Bainitic untempered steel were characterized by FEI QUANTA 450 scanning electron microscope (SEM). The microstructure of Bainitic untempered steel was observed by LEICA DMI8 inverted metallography microscope. Bruker D8 advance X-ray diffractometer (XRD) was used to obtain the diffraction spectra of Bainitic untempered steel. The hardness test was carried out by HVS-1000Z digital micro Vickers hardness testing machine of Shanghai Aolongxingdi Company. 10 points were randomly tested, and the Vickers hardness of the composite was obtained after the average value was taken. According to GB/T2 28.1-2010, the standard tensile specimen was processed, and the stress-strain curve was obtained by the electronic universal material testing machine (Z100A.THW)..

Table 1. Chemical composition of bainite-type non-quenched and tempered steels

element	C	Si	Mn	P	S	Cr	Ni	Mo	Al	V	Nb	Ti	N	B
content/%	0.19	0.12	2.7	0.02	0.01	0.84	0.04	0.08	0.032	0.06	0.02	0.04	0.03	0.0003

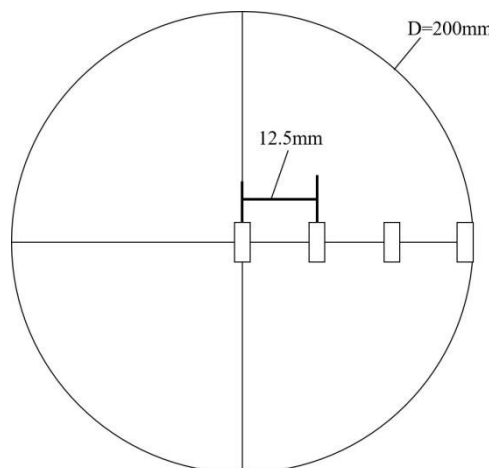


Fig.1 Schematic diagram of sampling

3. Experimental Results and Analysis

3.1 Microstructure Analysis

Fig. 2 is the OM diagram of the Bainitic untempered steel at different sampling locations. It can be seen from the OM diagram that the bainitic untempered steel has a variety of structures, mainly granular bainite, lat bainite and ferrite, and the ferrite is in block and strip shape. From the C-0 of the heart to the C-3 of the edge, it can be seen that the C-0 of the heart contains more granular bainite, but less lath bainite, the lath is the largest, the longest and the largest grain size. The content of granular bainite at C-1 and C-2 decreased, the content of lath bainite increased, the lath became thinner, the lath length and grain size decreased. The content of granular bainite and lath bainite decreased at C-3 of the edge, and the lath was the smallest, the length was the shortest, and the grain size was the smallest. At the same time, Image-Pro Plus software was used to calculate the average austenite grain size and ferritic content. The results are listed in Table 2, indicating that as the sampling position gets closer to the edge, the lath bainite content first increases and then decreases, the lath bainite lath becomes thinner, and the granular bainite content continuously decreases. This is mainly related to the cooling rate. Due to the large size of the large-diameter untempered bainitic steel, the cooling rate will be different in different positions during air cooling, and the core cooling rate will be slow, resulting in more granular bainite content, less lath bainite content, and longer and thicker lath length; As the sampling position gets closer and closer to the edge, the cooling rate increases continuously, resulting in the lath bainite content increasing first and then decreasing, the lath length and width decreasing continuously, while the granular bainite content decreasing continuously. The edge is mainly due to the larger ferrite content and size generated, resulting in the reduction of both lath bainite and granular bainite.

Table 2. Austenite grain average size and ferrite content

Equivalent diameter	C-0	C-1	C-2	C-3
Equivalent diameter/ μm	75.1	69.7	55.7	37.7
Ferrite content/%	4.2	8.4	10.7	15.8

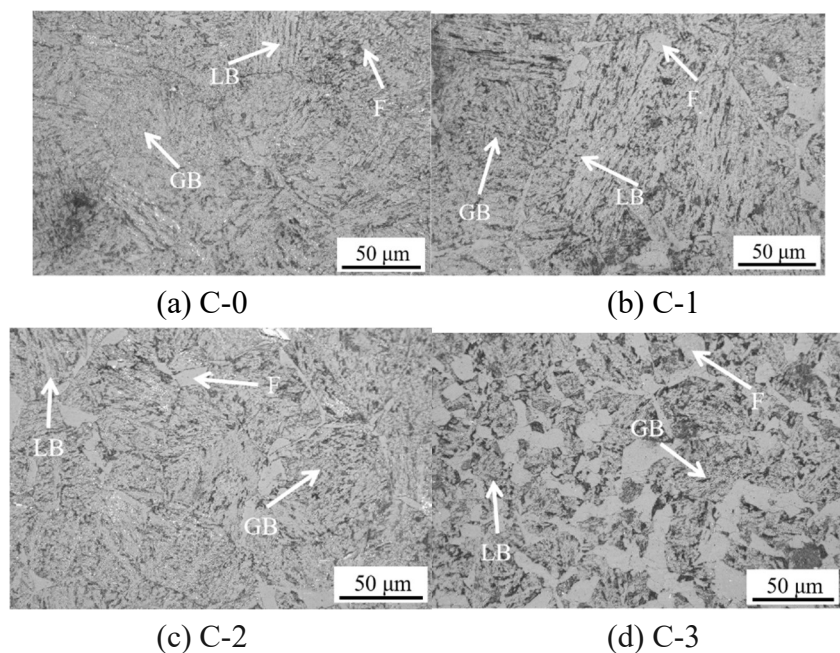


Fig. 2 Optical Micrographs at Different Sampling Positions. F, GB, and LB represent ferrite, granular bainite, and lath bainite, respectively

Fig. 3 shows the SEM images of Bainitic untempered steel at different sampling locations. It can be seen from Fig. 3 that the microstructure of Bainitic untempered steel is composed of lat bainite, granular bainite and ferrite, which is consistent with the results of metallograph. In C-0, C-1 and C-2, the ferrite content is small, and the ferrite size is small. In C-3, the ferrite content is large, and the ferrite size is large. At the same time, we can also see some small M/A islands and large massive M/A islands, as well as some decomposed M/A islands, mainly because high temperature tempering will cause M/A islands to decompose, reduce the strength of the material and improve the plasticity. At the same time, Image-Pro Plus was used to count 10 SEM images with 2000 times, and the average size of M/A island in the experimental steel was obtained, as shown in Fig. 4. It can be seen that the size of M/A island keeps decreasing as the sampling position gets closer to the edge. This is mainly due to the fact that during air cooling of untempered bainite steel, the larger the diameter, the different cooling rates at different locations and the larger the edge cooling rate. The lower the starting temperature of bainite transformation, the greater the driving force of phase transition, and the less sufficient the diffusion of carbon atoms, resulting in the fact that austenite can only enrich carbon within A short distance, the size of M/A island decreases, and the spacing is shortened^[13].

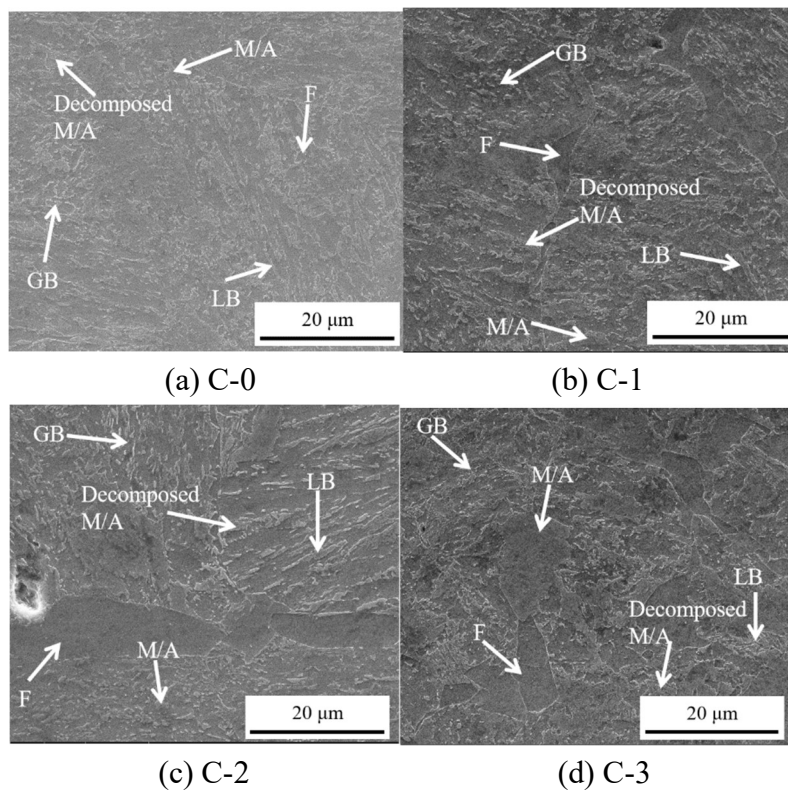


Fig. 3 SEM Images at Different Sampling Positions. F, M/A, GB, and LB represent ferrite, martensitic/austenitic islands, granular bainite, and lath bainite, respectively

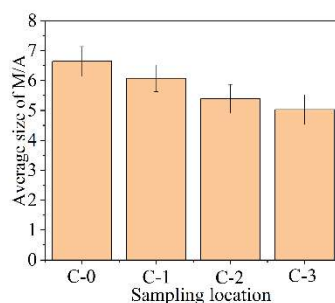


Fig. 4 The average size of island M/A at different sampling locations

3.2 Mechanical Properties Analysis

Fig. 5 shows the tensile stress-strain curve of Bainian type unmodulated steel. The results show that the tensile stress increases rapidly with the increase of strain, and decreases gradually after reaching the maximum value until fracture. At the same time, it is observed that the tensile strength of Bainitic untempered steel decreases at the edge.

Fig. 6 shows the relationship between the tensile strength, yield strength, elongation and sampling position of bainite non-quenched and tempered steel. As the sampling position is closer to the edge, the tensile strength and yield strength of bainite non-quenched and tempered steel first increase and then decrease, and the elongation decreases first and then increases. The tensile strength and yield strength reached the maximum values of 1050.3 MPa and 669.3 MPa when the sampling position was C-2, and the elongation reached the maximum value of 15 % when the sampling position was C-3 at the edge.

The change of tensile strength first depends on the relative content of granular bainite and lath bainite. According to the microstructure observation, from C-0 in the heart to C-3 at the edge, the content of lath bainite first increases and then decreases, while the content of granular bainite continuously decreases. Compared with granular bainite structure, lath bainite has a greater strengthening effect on low carbon steel, and the strength of lath bainite type low carbon steel is superior to that of granular bainite type low carbon steel^[14-15]. The tensile strength of low carbon steel increases with the increase of the volume fraction of lath bainite and M-A island^[16-17], so the tensile strength first increases and then decreases. Therefore, as the sampling position is closer to the edge, the tensile strength increases first and then decreases. The maximum tensile strength at C-2 is 1050.3 MPa, and the minimum tensile strength at C-0 is 950.1 MPa.

The change of yield strength first depends on the size of the grain. According to the grain statistics, as the sampling position gets closer to the edge, the grain becomes smaller, and the size of the grain determines the number of grain boundaries. At room temperature, the grain boundaries have an obstacle effect on sliding and affect the initial plastic deformation resistance of the experimental steel. According to the Hall-Petch formula^[18]:

$$\sigma_s = \sigma_0 + kd^{-1/2} \quad (1)$$

Where: σ_s is the yield strength of the polycrystal; d is the average grain diameter; σ_0 is the resistance to deformation in the crystal, equivalent to the yield strength of a very large single crystal; k is the influence coefficient of grain boundary on deformation, which is related to grain boundary structure^[19]. When the average grain diameter of the polycrystal decreases, the yield strength of the polycrystal will increase. Therefore, the yield strength is highest at C-2, but when the sampling position is the edge, the ferrite content is too much and the size is too large, resulting in a decrease in the yield strength of the edge.

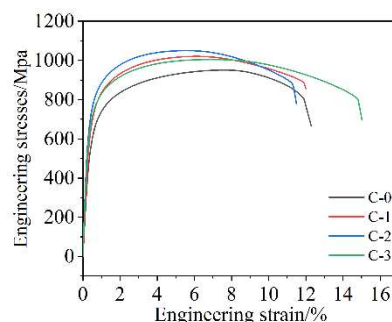


Fig. 5 Stress-Strain Curves at Different Sampling Positions

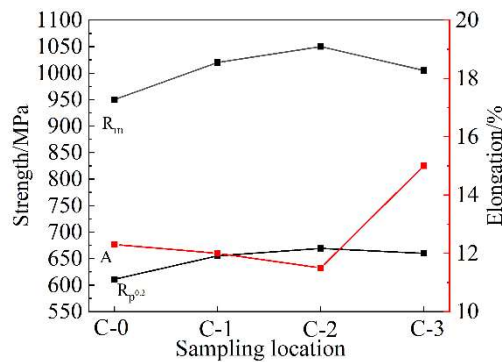


Fig. 6 Mechanical Performance Variation in Bainitic Non-Quenched and Tempered Steel

4. Conclusion

- (1) The microstructure of the bainite type non-quenched and tempered steel at different positions is granular bainite and lath bainite, and the bainite content of the lath increases first and then decreases as the sampling position gets closer to the edge, the lath bainite slats become thinner, the granular bainite content decreases, and the M/A island size and grain size decrease.
- (2) As the sampling position is closer to the edge, the tensile strength and yield strength of bainite non-quenched and tempered steel increase first and then decrease, and the elongation first decreases and then increases. The tensile strength and yield strength reached the maximum values of 1050.3 MPa and 669.3 MPa when the sampling position was C-2, and the elongation reached the maximum value of 15 % when the sampling position was C-3 at the edge.

References

- [1] Liu Jie, Wu Dan, Yang Xiujuan, et al. Research Status and Development Trend of untempered Steel [J]. Hot Working Technology, 2021, 50(23): 1-6+10.
- [2] Wang Zhanhua. Study on Microstructure and properties control of Bainitic untempered steels [D]. Beijing Jiaotong University, 2021.
- [3] Xie Weili, Shen Zhengyuan, Wu Huiqin et al. Mechanical Properties of untempered Steel and Their Application [J]. Heat Treatment, 2013, 28(04): 1-8.
- [4] Jiang Hongqing, Huang Xianliang, Huang Zhibing. Performance factors and Development status of untempered Steel [J]. Metal World, 2013, (05): 37-40.
- [5] Zhang Tuoyan, Yang Jun, Deng Ruigang. Research status and application of bainitic untempered steel [J]. Hot Working Technology, 2011, 40(08): 43-46.
- [6] Kang M Z, Jia H S, Yang Y Q, et al. New series quasi-bainitic steels [J]. Heat Treatment of Metals, 1995(12): 3-5.
- [7] Luo Zoming. Application and prospect of non-tempered steel [J]. Fujian Metallurgy, 2018(4): 52-56. (in Chinese).
- [8] Zhou Quan, Zhang Zheng, Wu Xiaochun, et al. Development of Large Section size SDP1 bainitic plastic Die Steel [J]. Materials for Mechanical Engineering, 2011, 35(S1): 91-94.
- [9] Luo Yi, Wu Xiaochun, Zhang Hongkui. Microstructure and properties of large section untempered prehardened plastic die Steel [J]. Heat Treatment of Metals, 2008, 33(3):28-31.
- [10] Fresh Fengqiang, Wang Zhilin, money Caillet, etc. Large size bayesian shape of non quenched and tempered steel XGMnVS development practice [J]. Journal of foundry technology, 2023, 44 (7) : 680-684. The DOI: 10.16410 / j.i ssn1000-8365.2023.2068.
- [11] Li Mengge, Cheng Juqiang, Yin Sibao. Microstructure and properties of untempered bainitic steels with different Section Sizes [J]. Heat Treatment of Metals, 2021, 46(08): 65-69. (in Chinese).

- [12] Wang Siqian, Zhang Zhonghe, Wang Feiyu, et al. Experimental study on Effect of Size Factors on Mechanical Properties of 35CrMoV Steel [J]. Heat Treatment Technology and Equipment, 2019, 40(02): 58-61.
- [13] Wei Junxiao, Guo Baoshun. Effect of cooling rate on microstructure and hardness of low carbon bainitic steel [J]. Modern Metallurgy, 2013, 41(04): 8-10.
- [14] ZHAO Yanqing, Sun Li, Liu Hongqiang et al. Effect of bainite Structure Type on Mechanical Properties of 780MPa grade low carbon bainite steel [J]. Hot Working Technology, 2019, 48(20): 148-150.
- [15] Yu Qingbo, Sun Ying, Ni Hongxin et al. Effects of Different types of bainite structures on Mechanical Properties of Low Carbon Steel [J]. Chinese Journal of Mechanical Engineering, 2009, 45(12): 284-288.
- [16] Han S Y, Sang Y S, Lee S, et al. Effect of cooling conditions on tensile and charpy impact properties of API X80 linepipe steels[J]. Metallurgical and Materials Transactions, 2010, 41A(2): 329.
- [17] Zhong Y, Xiao F, Zhang J, et al. In situ TEM study of the effect of M/A films at grain boundaries on crack propagation in an ultra-fine acicular ferrite pipeline steel[J]. Acta Materialia, 2006. 54(2): 435.
- [18] Hu Gengxiang, CAI Xun, Rong Yonghua. Fundamentals of Materials Science [M]. Shanghai: Shanghai Jiao Tong University Press, 2010: 183-190.
- [19] Shin S E, Choi H J, Shin J H, et al. Strengthening behavior of few-layered graphene/aluminum composites[J]. Carbon, 2015, 82: 143-151.